HHS Public Access

Author manuscript

Cancer Gene Ther. Author manuscript; available in PMC 2013 August 01.

Published in final edited form as:

Cancer Gene Ther. 2013 February ; 20(2): 109–116. doi:10.1038/cgt.2012.92.

Development of measles virus-based shielded oncolytic vectors: suitability of other paramyxovirus glycoproteins

Andrew W. Hudacek[1], **Chanakha K. Navaratnarajah**, and **Roberto Cattaneo**[*]

Department of Molecular Medicine, and Virology and Gene Therapy Track, Mayo Clinic College of Medicine, Rochester, Minnesota 55905

Abstract

Antibody-mediated neutralization may interfere with the efficacy of measles virus (MV) oncolysis. To circumvent vector neutralization, we sought to exchange the envelope glycoproteins, hemagglutinin (H) and fusion (F), with those from the non-cross reactive Tupaia paramyxovirus (TPMV). To sustain efficient particle assembly, we generated hybrid glycoproteins with the MV cytoplasmic tails and the TPMV ectodomains. Hybrid F-proteins that partially retained fusion function, and hybrid H-proteins that retained fusion support activity, were generated. However, when used in combination, the hybrid proteins did not support membrane fusion. An alternative strategy was developed based on a hybrid F protein and a truncated H protein that supported cell-cell fusion. A hybrid virus expressing these two proteins was rescued, and was able to spread by cell fusion, however was only capable of producing minimal amounts of particles. Lack of specific interactions between the matrix and the H-protein, in combination with sub-optimal F-protein processing and inefficient glycoprotein transport in the rescue cells, accounted for inefficient particle production. Ultimately, this interferes with applications for oncolytic virotherapy. Alternative strategies for the generation of shielded MV are discussed.

Keywords

Tupaia paramyxovirus; measles virus; glycoprotein modification; vector shielding

INTRODUCTION

Several viruses including Adeno-, Herpes-, Pox-, Reo- and Paramyxoviridae are being tested in clinical trials for the treatment of various tumors,[1, 2] and an oncolytic adenovirus is currently an approved cancer therapeutic in China.[3] However, the high prevalence of pre-existing antibodies against many vectors may reduce or eliminate their oncolytic efficacy.

[*]To whom correspondence should be addressed: Dr. Roberto Cattaneo, Mayo Clinic, Department of Molecular Medicine, 200 First Street SW, Rochester, MN 55905, USA, Phone +1 (507) 538-1188, Fax: +1 (507) 266-2122, Cattaneo.Roberto@mayo.edu.

[1]Current address: Department of Microbiology and Immunology, Jefferson Medical Collage, Thomas Jefferson University, Philadelphia, Pennsylvania 19107.

CONFLICT OF INTEREST

The authors declare no conflicts of interest.

This issue has been addressed by exchanging the envelope, or capsid, of different viruses with those of non-cross-reactive serotypes.[4, 5]

Measles virus (MV), one of the most promising oncolytic viruses, is currently used in phase I clinical trials to treat glioblastoma multiforme, multiple myeloma and ovarian cancer.[1, 6–8] Unlike other viruses such as vesicular stomatitis virus (VSV) and adenoviruses, MV has a single serotype.[9] Therefore a novel serotype was engineered based on the glycoprotein complex (the F and H proteins) from a related, but non-immunologically cross-reactive *Morbillivirus.*[10] This shielded MV remained oncolytic in an immunocompetent mouse model even in the presence of anti-MV neutralizing antibodies.[10] However, antibodies against the new envelope of the shielded MV will eventually be generated.

To allow for sequential cycles of virotherapy, additional shielding envelopes will need to be developed. Here, we investigated the suitability of the envelope glycoproteins from the *Tupaia paramyxovirus* (TPMV),[11, 12] a close relative of the *Morbillivirus* genus. While a direct exchange of the CDV and MV glycoproteins was possible,[10] our initial attempts to rescue a hybrid MV with the TPMV glycoproteins were unsuccessful (C. Springfeld and R. C., unpublished). Knowing that efficient MV particle assembly depends upon the interaction between the matrix protein and the cytoplasmic tails of the glycoproteins,[13, 14] and that the TPMV glycoprotein cytoplasmic tails are not homologous to the MV glycoprotein cytoplasmic tails, we then sought to generate hybrid glycoproteins. As the cytoplasmic tails of the TPMV glycoproteins are not characterized, we first generated truncation mutants and assessed fusion function. Based on this data, we generated hybrid glycoproteins with a TPMV ectodomain and the corresponding MV cytoplasmic tail. When associated with the wild-type partner, these hybrid glycoproteins retained high levels of fusion competency. However, in combination, hybrid F- and H-proteins no longer supported fusion.

On the other hand, the combination of a hybrid F-protein and a cytoplasmic tail-truncated TPMV H-protein sustained fusion function. A hybrid virus with these two proteins in place of MV F and H spread through cell-cell fusion, but failed to efficiently produce particles. We therefore sought to determine the factors influencing hybrid virus assembly by determining glycoprotein surface expression, transport and processing kinetics. We show that reduced hybrid F-protein processing and sub-optimal transport of glycoproteins in the virus producer cell line contribute to inefficient particle formation.

MATERIALS AND METHODS

Antibodies

Rabbit anti-TPMV-F_{ecto} was raised against the peptide NH_2-CELEMDKTQKALDRSNKIL-COOH, corresponding to amino acids 463 to 480 of the TPMV F protein (courtesy of C. Springfeld).[15] Rabbit anti-TPMV-H_{ecto} was raised against the KLH conjugated peptide NH_2-CSEDSTHDQGPGVEGTSRNHKGK-COOH, corresponding to amino acids 215 to 237 of the TPMV H protein. MV F- and H-protein were detected using rabbit antibodies against parts of their cytoplasmic tails: F_{cyt} [16, 17] and H_{cyt}.[18] The anti-H606 antibody recognizes the KLH conjugated peptide NH2-CTVTREDGTNSR-COOH corresponding to the terminal 12 residues of the MV-H protein.

AlexaFluor 647 goat anti-mouse and AlexaFluor 546 goat anti-rabbit (Invitrogen, Carlsbad, CA) secondary antibodies were used for immunofluorescence. Penta-His AlexaFluor 647 conjugated mouse monoclonal antibody (Qiagen, Valencia, CA) was used for the detection of 6xhis-tagged H proteins in confocal and FACS.

Plasmids

The plasmid pCG-IRESzeo was used for the expression of all deletion and chimeric glycoproteins.[19] The TPMV F and H cDNA were cloned from infected TBF cells using the following primers; BamHI-Ff (5′-AGCAGCATGCGGATCCATGGCATCACTGCTAAAAAC-3′), PacI-Fr (5′-AGCAGCATGCTTAATTAATTATCCACTTATATCTGTA-3′), BamHI-Hf (5′-AGCAGCATGCGGATCCATGGATTATCATTCACACAC-3′), and H6-HPacIr (5′-AGCAGCATGCTTAATTAATTAGTGGTGGTGGTGGTGGTGCTTAGTATTAGGACA TG-3′) (restriction sites are underlined) using the reverse transcriptase Superscript III (Invitrogen). DNAs coding for hybrid glycoproteins were generated by overlap extension PCR. Sequence verified clones were used to replace the F and H open reading frames in the full-length MV cDNA p(+)MVvac2(GFP)H, by exchange of *San*DI-*Pac*I (F) and *Pac*I-*Mlu*I (H) digested fragments to generate the hybrid virus p(+)MVvac2(FΔ32/mvcyt-HΔ90)GFP.[20] Primer sequences are available upon request.

The sequences of all glycoprotein genes, deletion mutants and hybrids were confirmed via DNA sequencing (ABI Prism 377 DNA sequencer; Perkin-Elmer Applied Biosystem, Waltham, MA). Full-length plasmids coding for a genomic cDNA conform to the rule-of-six.[21, 22]

Cells

Vero-αHis (African green monkey kidney Vero cells transduced to express a membrane bound single chain antibody recognizing a six-histidine tag),[23] Vero, 293 (human embryonic kidney) and TBF [24] cells were grown in Dulbecco's Modified Eagle's medium supplemented with 10% fetal calf serum (DMEM-10, Mediatech, Manassas, VA), 293-3-46 (MV rescue helper cell line) [25] were grown in DMEM-10 supplemented with 1.2mg/ml G418 (Invitrogen). CHO-K1 cells used in pulse-chase experiments were grown in DMEM-10 supplemented with non-essential amino acids (Mediatech). All cells were propagated at 37°C in a 5% CO_2 humidified incubator.

Viruses

The parental MVvac2(GFP)H [20] virus and derivatives were rescued, propagated and purified as described previously.[25] Briefly, 10μg of full-length DNA was transfected using the ProFection (Promega, Madison, WI) calcium phosphate transfection kit with 10 ng of the viral polymerase plasmid pEMC-La into 293-3-46 cells, which express the MV N and P proteins. Cells were plated at a density of 5×10^5 in 35 mm dishes and two days post-transfection, overlaid onto Vero-αHis cells. Cytopathic effect and GFP expression was monitored. The titers of the rescued viruses were determined by $\log_{10}$ 50% tissue culture infective dose ($TCID_{50}$) as calculated by the Spearman-Kärber method.[26, 27]

Virus growth kinetics

Cells were infected at an MOI of 0.03. At various time points, supernatant (media fractions) were clarified by centrifugation and cells were scraped into Opti-MEM I reduced-serum media (Invitrogen). The samples were rapidly frozen and thawed. Released and cell-associated viral titers were determined by $TCID_{50}$ titration.

Fusion assays

Cell-cell fusion assays were conducted using Vero-αHis cells plated at a density of 10^5 per well in 24-well tissue culture plates. The cells were transfected using Lipofectamine 2000 (Invitrogen) with expression plasmids pCG-TPMV F and pCG-TPMV $H_{His\text{-}tag}$ or its deletion mutants (0.4 μg/each). A plasmid expressing the green fluorescent protein (pEGFP-N1, 0.1 μg) was added to allow visualization of transfected cells. For each well the plasmid DNAs, 2μl of Lipofectamine 2000, 48μl of Opti-MEM were mixed; the mixture was let stand for 20 minutes at room temperature, and then added to cells for 24 hours. The extent of fusion was then recorded using the following convention: -, no syncytium; +, 3–5 nuclei per syncytium; ++, 5–15 nuclei per syncytium; +++, more than 15 nuclei per syncytium. Images were collected on a Nikon Eclipse TE300 using NIS-Elements F 3.0 software. Three fields of approximately 500 cells per field were scored and averaged. The fusion scores were based on the averages of at least three independent experiments.

Immunoblotting

Vero-αHis cells were plated and transfected as described for the cell-cell fusion assay. Samples were washed three times with PBS prior to cytoplasmic extraction using 100μl RIPA buffer (150mM NaCl, 1% Igepal CA-680, 0.5% sodium-deoxycholate, 0.1% SDS, 50mM Tris, pH 8) supplemented with protease inhibitor cocktail set I (Calbiochem, Rockland, MA) per well at 4°C for 5 minutes. The lysates were cleared by centrifugation at 21 000 x*g* for 10 minutes at 4°C. EndoH digestion was carried out on 10μl of cleared lysate. Protein samples were denatured using urea buffer [27] for 5 minutes at 95°C before separation on SDS-PAGE. Proteins were then transferred to polyvinylidine difluoride membranes (Immobilon-P, Millipore, Billerica, MA), blocked with 5% milk in TBST (10mM Tris, pH 8; 150mM NaCl; 0.05% Tween 20) and subjected to enhanced chemiluminescence detection using the antibodies indicated (GE Healthcare, Waukesha, WI).

FACS analysis

Cells were plated at 5×10^5 per 35mm dish and transfected as described above with 4 μg per well of either pCG-MV-H617, pCG-TPMV-$H_{His\text{-}tag}$, pCG-TPMV-HΔ90 or the negative control plasmid peGFP-N1. Twenty-four hours post-transfection, the cells were washed once with PBS and detached in 500μl Versene (Gibco) and washed with FACS buffer (PBS supplemented with 5% FCS and 0.1% NaN_3). Samples were stained with the anti-His specific antibody Penta-His AlexaFluor 647 (Qiagen) for one hour at 4°C, washed with FACS buffer and fixed with 2% paraformaldehyde in PBS. Samples were screened by the Mayo Clinic Optical Morphology Core facility and data was analyzed using FlowJo 9.4.10 software.

Metabolic labeling, immunoprecipitation and glycosidase digestion

CHO-K1 cells plated in 35mm dishes were transfected with 2μg F and $H_{His\text{-}tag}$ or mutant protein expression plasmids. Twenty-four hours post-transfection, cells were starved in cysteine- and methionine-deficient DMEM (Invitrogen, catalog number 21013-024) supplemented with sodium pyruvate, sodium bicarbonate and L-glutamate (DMEM -cys/-met) for 30 minutes, then labeled with Trans[^{35}S]-label (100μCi/ml) (Perkin Elmer) in DMEM -cys/-met for 1 hour at 37°C and chased with unlabeled DMEM-10 for the times indicated. Cells were then washed with PBS and lysed with 100μl denaturing lysis buffer (1% SDS, 50mM Tris, pH 7.5, 5mM EDTA, pH 8; for F protein) or 500μl RIPA buffer (for H proteins) supplemented with protease inhibitor (1mM PMSF and Protease inhibitor cocktail set 1). To expose the antigen recognized by the TPMV-F_{ecto} antibody, F protein samples were denatured at 99°C for 5 minutes followed by addition of 900μl of non-denaturing lysis buffer (1% Triton X-100, 50mM Tris, pH 7.5, 300mM NaCl, 0.02% sodium azide), and cell lysates were passed through a 25-gauge needle to shear genomic DNA. All lysates were then clarified by centrifugation for 20 minutes at 21 000 x*g*.

Aliquots of protein lysate were immunoprecipitated using the antibodies indicated with protein G-agarose (Roche, Indianapolis, IN) overnight at 4°C. The samples were washed and dissociated by boiling for 5 minutes in 0.5% SDS and 40mM DTT. Dissociated samples were then subjected to endo-β-*N*-acetylglycosaminidase H (EndoH, NEB, Ipswich, MA) digestion (20U/sample) at 37°C for 1 hour in 50mM sodium citrate, pH 5.5. H-protein samples were fractionated on 7.5% SDS-PAGE and F-proteins were fractionated on 10% SDS-PAGE. Protein band intensities were quantified using the Typhoon FLA 7000 phosphorimaging system and ImageQuant TL software (GE Healthcare).

RESULTS

TPMV H interacts with an unknown receptor present only on Tupaia cells.[12] Thus, to facilitate the functional analysis of hybrid proteins, we extended the TPMV H ectodomain with a six-histidine tag (His-tag). This His-tag allows us to utilize the Vero-αHis cell line, which expresses a pseudo-receptor recognizing it.[23, 28] These cells also support the rescue of retargeted MV-based vectors.[23]

TPMV F-protein with six amino acid cytoplasmic tail maintains wild-type fusion function

The TPMV F-protein cytoplasmic tail is 38 amino acids in length, 5 amino acids longer than the MV F-tail, with no homology shared between the two F-tails. Towards generating a chimeric F glycoprotein, we first sought to define the minimal sequence necessary for TPMV-F fusion function. We co-expressed the F and H glycoproteins in Vero-αHis cells and observed syncytia formation (Figure 1A).[28–30]

When the TPMV F-tail was shortened in ten amino acid increments (Figure 1B; FΔ10–FΔ40), we observed that deletion of up to 30 amino acids had no effect on fusion function (Figure 1B; FΔ10, FΔ20 and FΔ30, fusion score +++). When 40 amino acids were removed from the F-tail, we observed complete loss of fusion function (Figure 1B; FΔ40, fusion score -).

The protein expression levels of the F-tail truncation mutants were analyzed by separating cell lysates from transfected Vero-αHis cells and immunobloting with a TPMV F-ectodomain specific antibody (Figure 2A; Endo H - lanes). These analyses indicated that all the mutants were expressed at or near wild-type levels. Moreover, all mutant proteins retained proteolytic activation of the F_0 precursor to the fusion competent F_1+F_2 complex.

To define the minimal functional F-tail, we then shortened the F-tail in two amino acid increments (Figure 1B; FΔ32, FΔ34, FΔ36 and FΔ38). As FΔ32 was the largest truncation to still maintain wild-type fusion function, we selected this mutant for the generation of a hybrid F protein. This protein consists of the TPMV ectodomain, transmembrane domain, and 6 amino acids of the TPMV F-tail fused to the 33 amino acid MV F-tail (Figure 2B; FΔ32/mvcyt). When this hybrid F-protein was co-expressed with the standard TPMV H protein, it supported a slightly reduced level of fusion compared to the parental FΔ32 mutant (Figure 2B; fusion score ++).

TPMV H-protein with four-residue cytoplasmic tail maintains wild-type levels of fusion helper function

The TPMV H cytoplasmic tail is predicted to be 94-residues in length, ~60 residues longer than the MV H-tail. We made progressive truncations of the TPMV H-tail to define the minimal segment necessary for fusion-support function (Figure 3A; HΔ10–HΔ100). Up to 60 residues could be deleted without reducing fusion-support function (Figure 3A; mutants HΔ10–HΔ60, fusion scores of +++). Further truncations of 70 or 80 residues inhibited fusion-support function (Figure 3A; HΔ70 and HΔ80, fusion score ++). However, truncation of 90 residues restored normal function (Figure 3A; HΔ90, fusion score +++), while a deletion of 100 residues completely inhibited function (Figure 3A; HΔ100, fusion score -). The second round of truncations to further define the minimal functional H-tail thus included mutants HΔ92–HΔ98 (Figure 3A). With the exception of the HΔ92 mutant that had strongly reduced fusion-support function (Figure 3A; HΔ92, fusion score +), none of the additional mutants were fusion competent (Figure 3A; HΔ94–HΔ98). Therefore, the HΔ60 and HΔ90 mutants were considered the most promising for the generation of hybrid protein.

Next we documented H-protein expression by immunoblot analysis of cell lysates from Vero-αHis cells transfected with the respective H-protein constructs (Figure 3B). Comparable levels of H-protein expression were documented for HΔ20, HΔ30, HΔ40 and HΔ60 and wild type H. In contrast, HΔ10 and HΔ50 were expressed at much lower levels while retaining full fusion support, an observation indicating that high expression levels are not required for full function. As HΔ90 was the largest truncation to have maintained wild-type function and protein expression, we selected this mutant for the generation of a hybrid H protein.

We constructed a hybrid H-protein comprised of the ectodomain, transmembrane segment and three residues of the TPMV H-tail (HΔ90) fused to the 34-amino acid MV H-tail. The hybrid protein, which was named H 90/mvcyt supported fusion with slightly reduced efficiency when co-expressed with the wild-type TPMV F-protein (fusion score ++, data not shown). However, when HΔ90/mvcyt was co-expressed with the hybrid F protein, FΔ32/mvcyt, fusion was below detection levels, indicating that the combination of two hybrid

glycoproteins with slightly reduced fusion efficiency is not a viable option for virus rescue. To promote assembly while mitigating potential interference from the TPMV H-protein's bulky cytoplasmic segment, we paired the chimeric FΔ32/mvcyt with the truncated HΔ90, and found that this combination supported fusion with only slightly reduced efficiency (Figure 3C). We did not attempt to make a virus with the HΔ60deletion.

A TPMV-shielded hybrid MV propagates poorly

We then transferred the genes for the TPMV-MV F-protein hybrid and the truncated TPMV H-protein to the MV infectious cDNA,[20, 25] substituting the endogenous genes. We used the vaccine strain vector backbone p(+)MVvac2(GFP)H,[20] which expresses GFP as a marker protein, and named the hybrid virus MVvac2(FΔ32/mvcyt-HΔ90)GFP. This virus was recovered using the helper cell line 293-3-46 followed by propagation on Vero-αHis cells.[23, 25, 28] Green fluorescent infectious centers were observed in multiple experiments, and propagated for several passages. Following each passage cytopathic effect increased, until up to 80% of the cells were in syncytia. At this point, virus stocks were harvested, but found to have low titers usually ranging from 10^3 to 10^4 $TCID_{50}$/ml during early passages. Virus titer did not increase at late passages.

Nevertheless, we characterized the growth kinetics of the hybrid virus and compared it to the two parental viruses, MVvac2(GFP)H and TPMV (Figure 4). Titers of TPMV particles released from TBF cells reached 10^6 $TCID_{50}$/ml, with a ten-fold lower titer documented for cell-associated virus (Figure 4A). As expected, MV infectivity in Vero-αHis cells was predominantly cell-associated with titers reaching 10^6 $TCID_{50}$/ml, and cell-free titers approximately ten-fold lower (Figure 4B; filled symbols). However, growth analysis of the hybrid virus on Vero-αHis cells (Figure 4B; open symbols) revealed low intracellular titers of only 10^2 $TCID_{50}$/ml, and even lower extracellular titers.

Deletion of the TPMV H-protein cytoplasmic tail does not affect intracellular transport

As truncation of the cytoplasmic tail may affect intracellular transport, and thus particle assembly, we next characterized the efficiency of glycoprotein transport and processing.[5, 31] We first compared surface expression of wild type TPMV-H and HΔ90, and found low but comparable expression of the wild type and the truncated H-proteins on the surface of Vero-αHis cells (Figure 5, Vero-αHis column). A control cell line known to have optimal vesicular transport, CHO-K1, efficiently expressed both wild-type H and the truncated HΔ90 proteins at the cell surface (Figure 5, CHO-K1 column).

To more precisely compare intracellular transport of the wild type and truncated H proteins, we performed pulse-chase experiments to measure the acquisition of EndoH resistant glycans by the H-protein over time. The acquisition of EndoH resistance indicates conversion of high mannose glycans to hybrid and complex oligosaccharides following processing through the *medial*-Golgi apparatus.[32] We determined that 50% of the H proteins acquired EndoH resistance within 3 hours, reflecting transport through the *medial*-Golgi (Figure 6A and 6C; diamonds). A similar rate of transport was observed for HΔ90 (Figure 6B and 6C; squares). Thus, the truncation of the H-protein cytoplasmic tail does not hinder intracellular transport.

Modification of the TPMV F-protein tail affects proteolytic activation

We compared proteolytic activation of the wild type and chimeric TPMV F proteins by measuring the kinetics of F_0 cleavage by pulse-chase experiments. The efficiency of protein activation was determined by comparing the intensities of the F_0 and F_1 bands at different time points after adjusting for differences in signal intensities resulting from differential radiolabel incorporation between F_0 and F_1. We found that about 50% of the wt-F protein was activated in 6 hours (Figure 7A and 7C), while approximately 25% of FΔ32/mvcyt was activated during the same time period (Figure 7B and 7C). Thus, slow proteolytic processing of the hybrid F protein may contribute to inefficient particle production.

DISCUSSION

Antibody-mediated neutralization interferes with the efficacy of systemic virotherapy. To avoid MV-neutralizing antibodies, we previously shielded the MV nucleocapsid with the envelope glycoproteins from the related *Morbillivirus* CDV, and showed that this hybrid virus retains oncolytic efficacy.[10] To avoid the neutralizing response against the hybrid virus, and allow for sequential cycles of therapy, shielded viruses that are not cross-reactive with either the MV or CDV glycoproteins are required. Since all of the well-characterized members of the *Morbillivirus* genus are cross-reactive with one of these envelopes, we explored the suitability of the glycoproteins from the related TPMV for particle assembly. While a simple exchange of the MV and TPMV glycoproteins did not support virus rescue, but the combination of a hybrid F protein including the MV F cytoplasmic tail and a TPMV H protein with a truncated cytoplasmic tail did allow rescue. However, infectivity production was minimal: while we occasionally observed titers in the 10^5–10^6 $TCID_{50}$/ml in fresh supernatants, these titers dropped to 10^3 or lower after freeze-thawing. In practice, infectivity could be propagated only by cell fusion, limiting applications for oncolytic therapy.

We think that improper particle assembly is the limiting factor for the generation of stable particles of shielded MV: viral particles may not form properly, or be instable and fall apart after release from the cell. This implies that detailed information about the interactions required for MV particle assembly is necessary to design hybrid glycoproteins that better retain their fusion or fusion-support function. While the feasibility of envelope exchanges between members of the same Paramyxovirus genus is established,[33–35] and in one case glycoprotein exchange between viruses of different genera was successful when based on hybrid glycoproteins,[36] recent systematic studies have documented significant losses of fusion function for many hybrids paramyxovirus F proteins.[37] Analogously, we observed here that the TPMV-MV hybrid F protein lost some fusion function. Consistently with proposed multiple interactions between F and H at cell fusion, this negative effect was amplified when the hybrid F protein was expressed in combination with an H protein with a truncated cytoplasmic tail.

A promising strategy to adapt new shielding envelopes on oncolytic MV relies on the glycoproteins of recently characterized viruses[38, 39] and potential viruses.[40] Those kinds are more closely related to *Morbilliviruses* than TPMV, and their glycoproteins may be more easily adaptable to the MV nucleocapsid. In particular, we are exploring whether the

glycoproteins of feline morbillivirus, a very recently characterized member of the *Morbillivirus* genus,[41] retain efficient function and particle assembly, while at the same time not cross-reacting.

Having observed inefficient glycoprotein transport in Vero-αHis cells, we have tested other cell lines expressing anti-His tag pseudo-receptors as candidate hosts for virus rescue. These cell line include 293 H6,[42] U118MG-HissFv.rec[43, 44] and CHO-αHis,[23] which have been used for the rescue of other viruses. Both U118MG-HissFv.rec[43, 44] and CHO-αHis[23] transport MV and TPMV H with approximately 3-times greater efficiency than Vero-αHis (data not shown). As the former cells are of human origin, they may be better hosts for the recovery of shielded recombinant MV than Vero-αHis cells.

Finally, truncated TPMV glycoproteins have recently been utilized for the shielding of lentivirus-based vectors,[15] specifically FΔ32 and HΔ80 truncated mutants to effectively package lentiviral capsids.[15] We note that the lentiviral *gag*-protein contains sequences that promote budding referred to as late domains,[45, 46] and that these capsid do not depend on specific interactions for budding. This mechanism may mitigate the effects of the reduced fusion phenotype on infectivity and particle production. In contrast to the lentiviral system, late domains have not been identified in MV proteins.

Acknowledgments

We thank Dr. Christoph Springfeld for providing the TPMV-F_{ecto} antibody and helpful insights into previously attempted envelope exchanges. We thank Dr. Stephen Russell for providing the Vero-αHis cell line, and Dr. Patricia Devaux for numerous helpful discussions. This work was supported by NIH RO1 CA 139389. The salary of AWH was provided in part by the Mayo Graduate School.

References

1. Cattaneo R, Miest T, Shashkova EV, Barry MA. Reprogrammed viruses as cancer therapeutics: targeted, armed and shielded. Nat Rev Microbiol. 2008; 6:529–40. [PubMed: 18552863]
2. Liu TC, Galanis E, Kirn D. Clinical trial results with oncolytic virotherapy: a century of promise, a decade of progress. Nat Clin Pract Oncol. 2007; 4:101–117. [PubMed: 17259931]
3. Garber K. China approves world's first oncolytic virus therapy for cancer treatment. J Natl Cancer Inst. 2006; 98:298–300. [PubMed: 16507823]
4. Parks R, Evelegh C, Graham F. Use of helper-dependent adenoviral vectors of alternative serotypes permits repeat vector administration. Gene Ther. 1999; 6:1565–1573. [PubMed: 10490766]
5. Rose JK, Bergmann JE. Altered cytoplasmic domains affect intracellular transport of the vesicular stomatitis virus glycoprotein. Cell. 1983; 34:513–24. [PubMed: 6352053]
6. Galanis E, Hartmann LC, Cliby WA, Long HJ, Peethambaram PP, Barrette BA, et al. Phase I trial of intraperitoneal administration of an oncolytic measles virus strain engineered to express carcinoembryonic antigen for recurrent ovarian cancer. Cancer Res. 2010; 70:875–82. [PubMed: 20103634]
7. Msaouel P, Dispenzieri A, Galanis E. Clinical testing of engineered oncolytic measles virus strains in the treatment of cancer: an overview. Curr Opin Mol Ther. 2009; 11:43–53. [PubMed: 19169959]
8. Russell SJ, Peng KW. Measles virus for cancer therapy. Curr Top Microbiol Immunol. 2009; 330:213–241. [PubMed: 19203112]
9. Griffin, DE. Measles Virus. In: Fields, B.; Knipe, DM.; Howley, PM., editors. Fields' Virology. 5. Vol. 1. Lippincott Williams and Wilkins; Philadelphia: 2007. p. 1551-1585.

10. Miest TS, Yaiw KC, Frenzke M, Lampe J, Hudacek AW, Springfeld C, et al. Envelope-chimeric entry-targeted measles virus escapes neutralization and achieves oncolysis. Mol Ther. 2011; 19:1813–20. [PubMed: 21610701]
11. Tidona CA, Kurz HW, Gelderblom HR, Darai G. Isolation and molecular characterization of a novel cytopathogenic paramyxovirus from tree shrews. Virology. 1999; 258:425–34. [PubMed: 10366580]
12. Springfeld C, von Messling V, Tidona CA, Darai G, Cattaneo R. Envelope targeting: hemagglutinin attachment specificity rather than fusion protein cleavage-activation restricts Tupaia paramyxovirus tropism. J Virol. 2005; 79:10155–10163. [PubMed: 16051808]
13. Cathomen T, Mrkic B, Spehner D, Drillien R, Naef R, Pavlovic J, et al. A matrix-less measles virus is infectious and elicits extensive cell fusion: consequences for propagation in the brain. Embo J. 1998; 17:3899–908. [PubMed: 9670007]
14. Cathomen T, Naim HY, Cattaneo R. Measles viruses with altered envelope protein cytoplasmic tails gain cell fusion competence. J Virol. 1998; 72:1224–1234. [PubMed: 9445022]
15. Enkirch T, Kneissl S, Hoyler B, Ungerechts G, Stremmel W, Buchholz CJ, et al. Targeted lentiviral vectors pseudotyped with the Tupaia paramyxovirus glycoproteins. Gene Ther. 2012
16. Spielhofer P, Bachi T, Fehr T, Christiansen G, Cattaneo R, Kaelin K, et al. Chimeric measles viruses with a foreign envelope. J Virol. 1998; 72:2150–9. [PubMed: 9499071]
17. Hu A, Cathomen T, Cattaneo R, Norrby E. Influence of N-linked oligosaccharide chains on the processing, cell surface expression and function of the measles virus fusion protein. J Gen Virol. 1995; 76:705–10. [PubMed: 7897359]
18. Funke S, Maisner A, Muhlebach MD, Koehl U, Grez M, Cattaneo R, et al. Targeted cell entry of lentiviral vectors. Mol Ther. 2008; 16:1427–36. [PubMed: 18578012]
19. Cathomen T, Buchholz CJ, Spielhofer P, Cattaneo R. Preferential initiation at the second AUG of the measles virus F mRNA: a role for the long untranslated region. Virology. 1995; 214:628–32. [PubMed: 8553566]
20. Reyes-del Valle J, Devaux P, Hodge G, Wegner NJ, McChesney MB, Cattaneo R. A vectored measles virus induces hepatitis B surface antigen antibodies while protecting macaques against measles virus challenge. J Virol. 2007; 81:10597–605. [PubMed: 17634218]
21. Rager M, Vongpunsawad S, Duprex WP, Cattaneo R. Polyploid measles virus with hexameric genome length. Embo J. 2002; 21:2364–72. [PubMed: 12006489]
22. Calain P, Roux L. The rule of six, a basic feature for efficient replication of Sendai virus defective interfering RNA. J Virol. 1993; 67:4822–30. [PubMed: 8392616]
23. Nakamura T, Peng KW, Harvey M, Greiner S, Lorimer IA, James CD, et al. Rescue and propagation of fully retargeted oncolytic measles viruses. Nat Biotechnol. 2005; 23:209–14. [PubMed: 15685166]
24. Darai G, Matz B, Flugel RM, Grafe A, Gelderblom H, Delius H. An adenovirus from Tupaia (tree shrew): growth of the virus, characterization of viral DNA, and transforming ability. Virology. 1980; 104:122–38. [PubMed: 6156536]
25. Radecke F, Spielhofer P, Schneider H, Kaelin K, Huber M, Dotsch C, et al. Rescue of measles viruses from cloned DNA. Embo J. 1995; 14:5773–84. [PubMed: 8846771]
26. Karber G. Beitrag zur kollektiven Behandlung pharmakologischer Reihenversuche. Arch Exp Pathol Pharmakol. 1931; 162:480–483.
27. Devaux P, von Messling V, Songsungthong W, Springfeld C, Cattaneo R. Tyrosine 110 in the measles virus phosphoprotein is required to block STAT1 phosphorylation. Virology. 2007; 360:72–83. [PubMed: 17112561]
28. Nakamura T, Peng KW, Vongpunsawad S, Harvey M, Mizuguchi H, Hayakawa T, et al. Antibody-targeted cell fusion. Nat Biotechnol. 2004; 22:331–6. [PubMed: 14990955]
29. Navaratnarajah CK, Vongpunsawad S, Oezguen N, Stehle T, Braun W, Hashiguchi T, et al. Dynamic interaction of the measles virus hemagglutinin with its receptor signaling lymphocytic activation molecule (SLAM, CD150). J Biol Chem. 2008; 283:11763–71. [PubMed: 18292085]
30. Vongpunsawad S, Oezgun N, Braun W, Cattaneo R. Selectively receptor-blind measles viruses: Identification of residues necessary for SLAM- or CD46-induced fusion and their localization on a new hemagglutinin structural model. J Virol. 2004; 78:302–13. [PubMed: 14671112]

31. Bagai S, Lamb RA. Truncation of the COOH-terminal region of the paramyxovirus SV5 fusion protein leads to hemifusion but not complete fusion. J Cell Biol. 1996; 135:73–84. [PubMed: 8858164]
32. Tarentino AL, Trimble RB, Plummer TH Jr. Enzymatic approaches for studying the structure, synthesis, and processing of glycoproteins. Methods Cell Biol. 1989; 32:111–39. [PubMed: 2691848]
33. Buchholz UJ, Granzow H, Schuldt K, Whitehead SS, Murphy BR, Collins PL. Chimeric bovine respiratory syncytial virus with glycoprotein gene substitutions from human respiratory syncytial virus (HRSV): effects on host range and evaluation as a live-attenuated HRSV vaccine. J Virol. 2000; 74:1187–99. [PubMed: 10627529]
34. Stope MB, Karger A, Schmidt U, Buchholz UJ. Chimeric bovine respiratory syncytial virus with attachment and fusion glycoproteins replaced by bovine parainfluenza virus type 3 hemagglutinin-neuraminidase and fusion proteins. J Virol. 2001; 75:9367–77. [PubMed: 11533200]
35. Tao T, Durbin AP, Whitehead SS, Davoodi F, Collins PL, Murphy BR. Recovery of a fully viable chimeric human parainfluenza virus (PIV) type 3 in which the hemagglutinin-neuraminidase and fusion glycoproteins have been replaced by those of PIV type 1. J Virol. 1998; 72:2955–2961. [PubMed: 9525616]
36. Tao T, Skiadopoulos MH, Davoodi F, Riggs JM, Collins PL, Murphy BR. Replacement of the ectodomains of the hemagglutinin-neuraminidase and fusion glycoproteins of recombinant parainfluenza virus type 3 (PIV3) with their counterparts from PIV2 yields attenuated PIV2 vaccine candidates. J Virol. 2000; 74:6448–6458. [PubMed: 10864657]
37. Zokarkar A, Lamb RA. The paramyxovirus fusion protein C-terminal region: mutagenesis indicates an indivisible protein unit. J Virol. 2012; 86:2600–9. [PubMed: 22171273]
38. Renshaw RW, Glaser AL, Van Campen H, Weiland F, Dubovi EJ. Identification and phylogenetic comparison of Salem virus, a novel paramyxovirus of horses. Virology. 2000; 270:417–29. [PubMed: 10793001]
39. Chua KB, Wang LF, Lam SK, Crameri G, Yu M, Wise T, et al. Tioman virus, a novel paramyxovirus isolated from fruit bats in Malaysia. Virology. 2001; 283:215–29. [PubMed: 11336547]
40. Drexler JF, Corman VM, Muller MA, Maganga GD, Vallo P, Binger T, et al. Bats host major mammalian paramyxoviruses. Nat Commun. 2012; 3:796. [PubMed: 22531181]
41. Woo PC, Lau SK, Wong BH, Fan RY, Wong AY, Zhang AJ, et al. Feline morbillivirus, a previously undescribed paramyxovirus associated with tubulointerstitial nephritis in domestic cats. Proc Natl Acad Sci U S A. 2012; 109:5435–40. [PubMed: 22431644]
42. Grandi P, Wang S, Schuback D, Krasnykh V, Spear M, Curiel DT, et al. HSV-1 virions engineered for specific binding to cell surface receptors. Mol Ther. 2004; 9:419–27. [PubMed: 15006609]
43. van den Wollenberg DJ, van den Hengel SK, Dautzenberg IJ, Cramer SJ, Kranenburg O, Hoeben RC. A strategy for genetic modification of the spike-encoding segment of human reovirus T3D for reovirus targeting. Gene Ther. 2008; 15:1567–78. [PubMed: 18650851]
44. Douglas JT, Miller CR, Kim M, Dmitriev I, Mikheeva G, Krasnykh V, et al. A system for the propagation of adenoviral vectors with genetically modified receptor specificities. Nat Biotechnol. 1999; 17:470–5. [PubMed: 10331807]
45. Rauch S, Martin-Serrano J. Multiple interactions between the ESCRT machinery and arrestin-related proteins: implications for PPXY-dependent budding. J Virol. 2011; 85:3546–56. [PubMed: 21191027]
46. Chen BJ, Lamb RA. Mechanisms for enveloped virus budding: can some viruses do without an ESCRT? Virology. 2008; 372:221–32. [PubMed: 18063004]

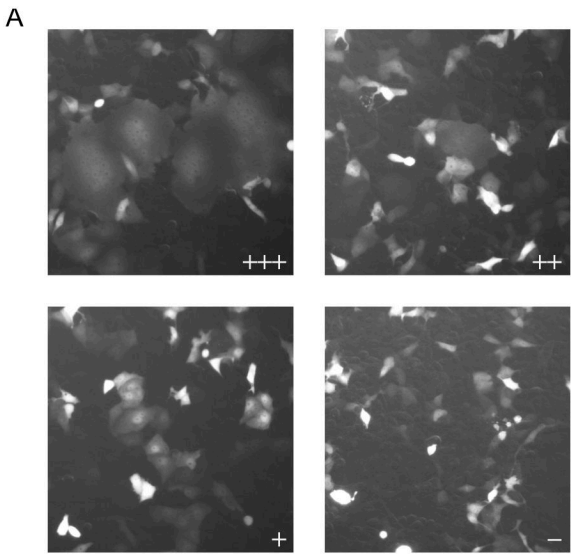

B

	TM	CT	Fusion
F	LFGVSYYAF	KIWSKLHFLDSYVYSLRNPSHHRSNGHQNHSFSTDISG*	+++
FΔ10	LFGVSYYAF	KIWSKLHFLDSYVYSLRNPSHHRSNGHQ*	+++
FΔ20	LFGVSYYAF	KIWSKLHFLDSYVYSLRN*	+++
FΔ30	LFGVSYYAF	KIWSKLHF*	+++
FΔ32	LFGVSYYAF	KIWSKL*	+++
FΔ34	LFGVSYYAF	KIWS*	+
FΔ36	LFGVSYYAF	KI*	++
FΔ38	LFGVSYYAF	*	++
FΔ40	LFGVSYY*		-

Figure 1.

Functional characterization of TPMV F proteins with truncations of the cytoplasmic tail. (A) Examples of visual assessment of syncytium formation. Cells were co-transfected with a standard or mutated F-expression plasmids, the standard H-expression plasmid, and a GFP-expression plasmid. The fusion score was assessed 24-hours after transfection. The F-plasmids used for the four examples are: FΔ32 (fusion score: +++), FΔ38 (fusion score: ++), FΔ34 (fusion score: +) and FΔ40 (fusion score: -). (B) Sequence of the F-protein predicted cytoplasmic tail (CT) and part of the transmembrane (TM) segment; a vertical line separates the two regions. Deletion mutants were named by their extent, such as a deletion of 10 amino acids was named FΔ10. The fusion efficiency of each construct was tested after co-expression with the standard $H_{His\text{-}tag}$ protein. The ectodomain of this protein is extended with a six-histidine tag, allowing for fusion-support function in Vero-αHis cells, expressing a pseudo-receptor recognizing the His-tag [23, 28]. Fusion efficiently levels are denoted on the right using the scale illustrated in panel A.

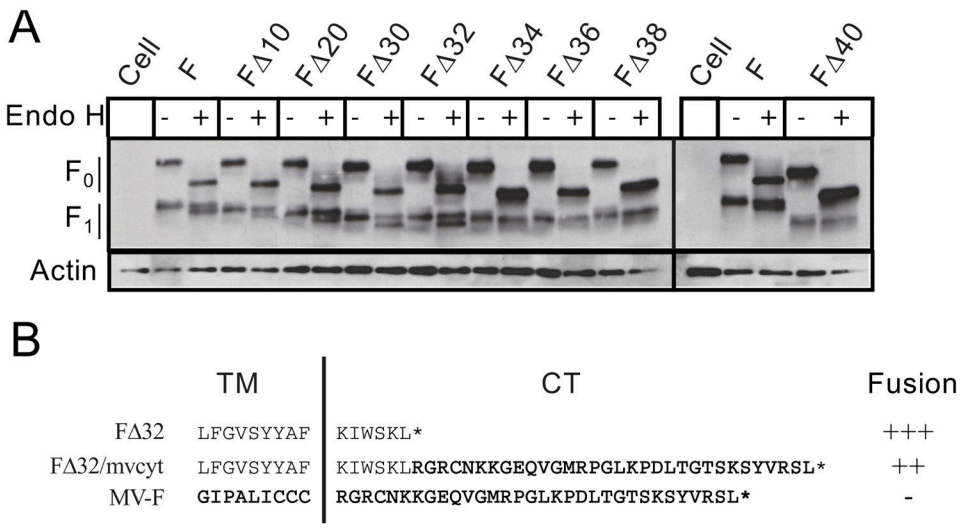

Figure 2.

Biochemical and functional characterization of F protein mutants. (A) Protein expression analysis. Cell lysates from transfected Vero-αHis cells used to assess fusion function were digested without or with EndoH (−/+), fractionated on 10% SDS-PAGE, and immunoblotted with a TPMV F specific antibody (F_{ecto}, upper panel). F_0: precursor protein, F_1: larger portion of the active F molecule (upper panel), actin: cellular actin (lower panel). (B) Schematic representation of the FΔ32 deletion mutant and the hybrid glycoprotein FΔ32/mvcyt (MV amino acids are bold typeface and underlined). Fusion scores are indicated with the same convention as in Figure 1.

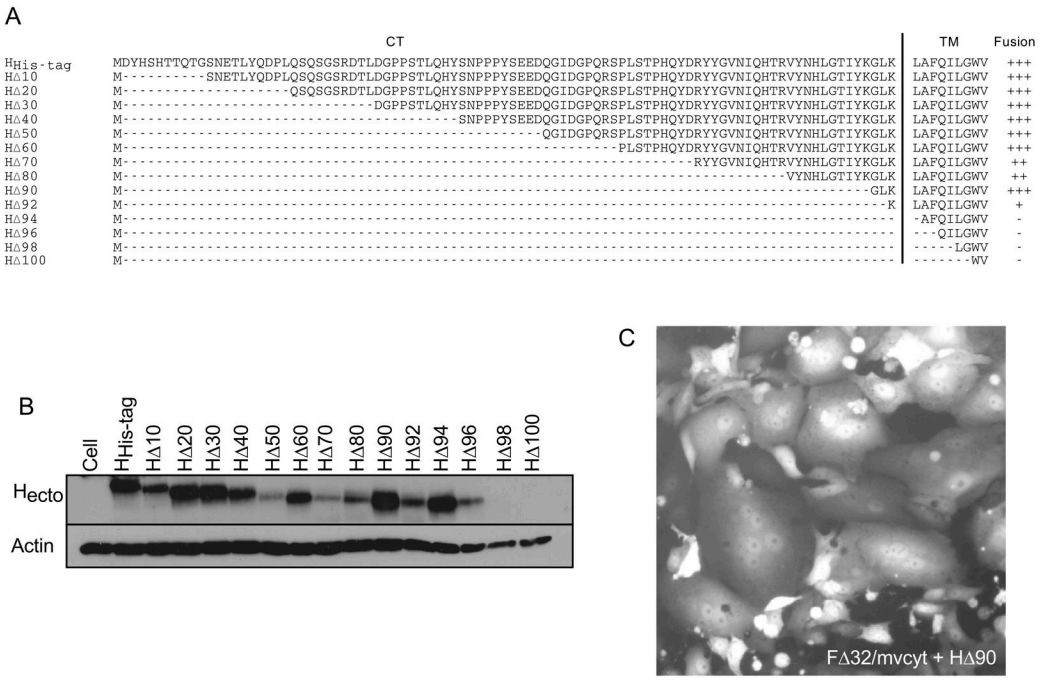

Figure 3.

Functional and biochemical characterization of H protein cytoplasmic tail truncations. (A) Sequence of the predicted 94 residue cytoplasmic tail (CT) and part of the transmembrane (TM) region; the two regions are separated by a vertical line. H protein deletions were named for the extent of their truncation, such that an H protein with a CT truncation of 10 amino acids was named HΔ10. The fusion efficiency of each construct when co-expressed with the full-length F protein in Vero-αHis cells is indicated on the right by the same convention outlined in figure 1. (B) H-protein expression analysis. Cell lysates were collected and fractioned on 7.5% SDS-PAGE and probed with the TPMV H specific antibody H_{ecto} (upper panel) or for cellular actin (lower panel). (C) Fusion of Vero-αHis cells after co-transfection of plasmids expressing FΔ32/mvcyt and HΔ90. A co-transfected plasmid expressing GFP allows for visualization of transfected cells. Cells were observed 24 hours after the beginning of transfection.

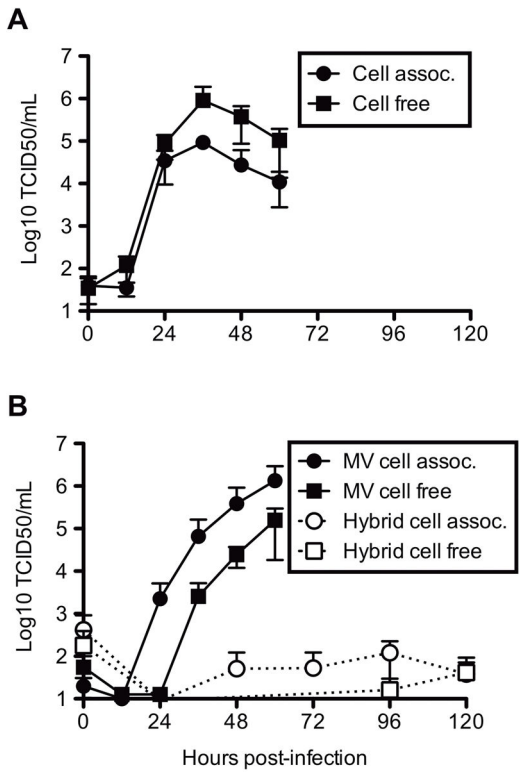

Figure 4.

Time course of cell-associated and cell-free virus production. Growth analysis of (A) TPMV in TBF cells, (B) MVvac2(GFP)N and MVvac2(FΔ32/mvcyt-HΔ90)GFP in Vero-αHis cells. All viruses were inoculated at an MOI of ~0.03. Titers were determined by collection of cellular (circles) and supernatant (squares) fractions every 12 hours over a 60 hour time period for TPMV and MV (filled symbols), and every 24 hours over a 120-hour time period for the hybrid virus (open symbols). Vertical axis: titer by $TCID_{50}$/ml, horizontal axis: time post-infection.

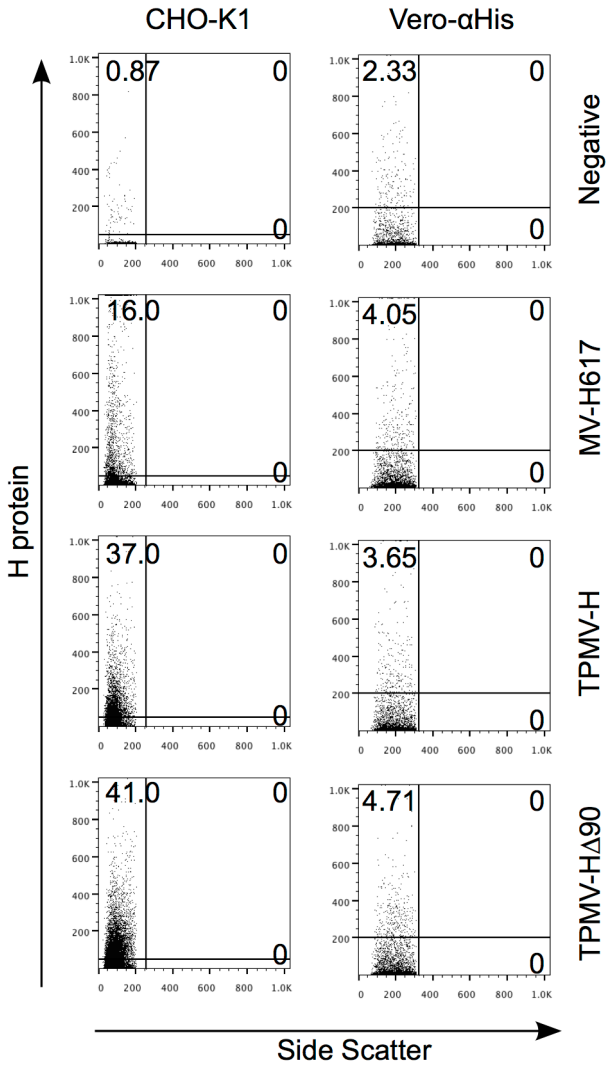

Figure 5.

FACS analysis of surface expression of MV and TPMV glycoproteins in CHO-K1 and Vero-αHis cells. Cells were mock-transfected (negative) or transfected with the plasmids encoding MV-H617, TPMV-$H_{His\text{-}tag}$ or TPMV-H 90. After 24 hours, cells were stained with anti-Penta-His AlexaFluor 647 conjugated antibody.

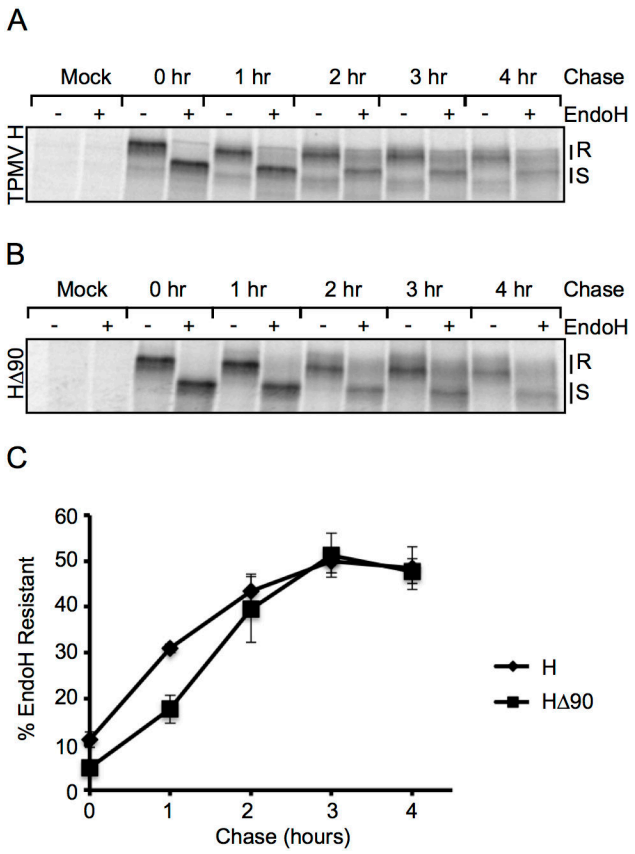

Figure 6.

Wild-type and truncated TPMV H protein transport kinetics. CHO-K1 cells were transfected with wild-type F and (A) $H_{His\text{-}tag}$ or (B) H 90 or an empty vector (mock) for 24 hours before being starved for 30 minutes and pulsed with 100μCi/ml ^{35}S labeled methionine and cysteine for 1 hour and then chased for up to 4 hours. After the indicated chase period, cell lysates were collected and H was immunoprecipitated and digested without or with EndoH (−/+ lanes, respectively) followed by fractioning on 7.5% SDS-PAGE. (C) Kinetics of complex oligosaccharide acquisition. Vertical axis: percent EndoH resistance of three experiments for wild type H (diamonds) and HΔ90 (squares). Horizontal axis: time of chase (hours).

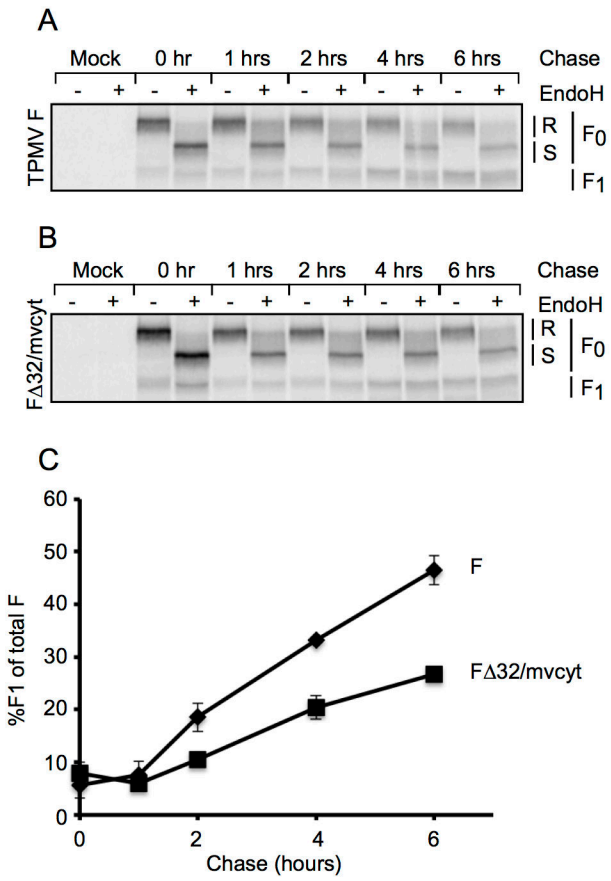

Figure 7.

Processing kinetics of TPMV F and FΔ32/mvcyt hybrid proteins. (A and B) SDS-PAGE analysis. CHO-K1 cells were transfected with TPMV $H_{His\text{-}tag}$ and either wild-type TPMV F (A), FΔ32/mvcyt (B), or an empty vector (mock in A and B), for 24 hours before being starved for 30 minutes and pulsed with 100μCi/ml ^{35}S labeled methionine and cysteine for 1 hour, then chased for up to 6 hours. Cellular lysates were collected at the indicated times and F protein was immunoprecipitated and digested without or with EndoH (−/+ lanes, respectively) followed by fractioning on 10% SDS-PAGE. The positions of F_0 and F_1 are indicated on the right. R: EndoH resistant band. S: EndoH sensitive band. (C) Kinetics of F-protein processing. The quantity of F_1 protein was measured in three independent experiments. Wild-type F: diamonds, FΔ32/mvcyt: squares. Vertical axis: percentage of F-protein processed. Horizontal axis: time of chase (hours).